

Linking high- z and low- z : Are We Observing the Progenitors of the Milky Way with JWST?

ELKA RUSTA,^{1,2} STEFANIA SALVADORI,^{1,2} VIOLA GELLI,^{3,4} IOANNA KOUTSOURIDOU,^{1,2} AND ALESSANDRO MARCONI^{1,2}

¹*Dipartimento di Fisica e Astronomia, Università degli Studi di Firenze, Largo E. Fermi 1, 50125, Firenze, Italy*

²*INAF/Osservatorio Astrofisico di Arcetri, Largo E. Fermi 5, 50125, Firenze, Italy*

³*Cosmic Dawn Center (DAWN), Denmark*

⁴*Niels Bohr Institute, University of Copenhagen, Jagtvej 128, 2200 Copenhagen N, Denmark*

Abstract

The recent JWST observation of the *Firefly Sparkle* at $z = 8.3$ offers a unique opportunity to link the high- and the low- z Universe. Indeed, the claim of it being a Milky Way (MW) type of assembly at the cosmic dawn opens the possibility of interpreting the observation with locally calibrated galaxy-formation models. Here, we use the MW-evolution model NEFERTITI to perform forward modeling of our Galaxy’s progenitors at high- z . We build a set of mock spectra for the MW building blocks to make predictions for JWST and to interpret the *Firefly Sparkle* observation. First, we find that the most massive MW progenitor becomes detectable in a deep survey like JADES from $z \approx 8.2$, meaning that we could have already observed MW-analogs that still need interpretation. Second, we provide predictions for the number of detectable MW progenitors in lensed surveys like CANUCS, and interpret the *Firefly Sparkle* as a group of MW building blocks. Both the number of detections and the observed NIRCcam photometry are consistent with our predictions. By identifying the MW progenitors whose mock photometry best fits the data, we find bursty and extended star-formation histories, lasting $> 150 - 300$ Myr, and estimate their properties: $M_h \approx 10^{8-9} M_\odot$, $M_* \approx 10^{6.2-7.5} M_\odot$, $SFR \approx 0.04 - 0.20 M_\odot yr^{-1}$ and $Z_{gas} \approx 0.04 - 0.24 Z_\odot$. Uncovering the properties of MW-analogs at cosmic dawn by combining JWST observations and locally-constrained models, will allow us to understand our Galaxy’s formation, linking the high- and low- z perspectives.

Keywords: galaxies: high-redshift — galaxies: evolution — galaxies: formation

1. INTRODUCTION

The galaxies that populate the present-day Universe, such as our own Milky Way (MW), are predicted to result from the hierarchical assembling of lower-mass progenitor galaxies, some of which formed > 13 billion years ago (e.g. White & Rees 1978; Tumlinson 2010; Salvadori et al. 2010). During the last decade, our knowledge of the MW in its present state has tremendously advanced thanks to local stellar surveys (e.g., Gaia, Gaia Collaboration et al. 2023, GALAH, Buder et al. 2021). Furthermore, observations of ancient metal-poor stars (e.g. Bonifacio et al. 2021) are providing key insights on the early stages of the MW evolution, which can be used to indirectly study the formation of the MW and

constrain cosmological models (e.g. Hartwig et al. 2022; Koutsouridou et al. 2023). However, we lack an understanding of how to link our knowledge of present-day galaxies with those observed at high- z .

The exceptional capability of the *James Webb Space Telescope* (JWST) has opened the possibility of looking directly at the early stages of galaxy formation. Several surveys (e.g. GLASS, Treu et al. 2022; JADES, Eisenstein et al. 2023; CEERS, Finkelstein et al. 2023) have been designed to observe galaxies at the so-called cosmic dawn (redshift $z \approx 15 - 6$) and many bright galaxies have been already discovered and spectroscopically confirmed at $z > 10$ (e.g. Harikane et al. 2023, 2024; Carniani et al. 2024). Moreover, gravitational lensing enabled to catch the light of fainter and lower-mass galaxies that would otherwise be inaccessible in the early Universe (e.g. Roberts-Borsani et al. 2023; Vanzella et al. 2023).

Ultimately, we are accumulating large amounts of data for both present-day and high- z galaxies. Still, we need

to connect these two regimes to understand the overall galaxy-formation process.

Very recently, the JWST CANadian NIRISS Unbiased Cluster Survey program (CANUCS, Willott et al. 2022) has provided a unique opportunity to fill this gap by reporting the discovery of a strongly lensed system at $z = 8.3$, the *Firefly Sparkle* (Mowla et al. 2024). The Firefly Sparkle comprises 10 systems identified as “star clusters” and it has two neighboring galaxies at ≈ 2 kpc and ≈ 13 kpc. By comparing the stellar masses derived for these systems with those predicted by abundance matching methods, the authors suggest to have observed a MW-like assembly.

However physical properties of distant galaxies, such as the Firefly Sparkle systems, are inferred from photometric data through spectral energy distribution (SED) fitting. Inferring the star-formation histories (SFH) of galaxies becomes particularly challenging at high- z due to their bursty nature. Indeed, both simulations (e.g. Sun et al. 2023; Pallottini & Ferrara 2023; Gelli et al. 2023) and recent JWST observations (e.g. Endsley et al. 2023; Langeroodi & Hjorth 2024; Looser et al. 2023) are revealing that in the first billion years of the Universe, galaxies undergo complex and highly time-variable evolution, difficult to capture through SED fitting techniques. Observing the building blocks of the MW at high- z might allow us to solve this issue. In this case, indeed, we can interpret the observed SEDs by exploiting locally-calibrated MW-formation models to obtain physically-founded SFHs.

In this letter, we interpret the Firefly Sparkle observation using a forward modeling approach based on the predictions of NEFERTITI, a data-calibrated model for the MW formation (Koutsouridou et al. 2023). We aim to answer the following questions: Is the Firefly Sparkle consistent with a MW-like analog at $z \approx 8$? And if so, what are the properties of the observed MW progenitors? By comparing our predicted SEDs with those observed in the Firefly Sparkle we will link the low- and high- z Universe, also providing key predictions to unveil other infant MW-like galaxies with the JWST.

2. METHODS

The forward modeling approach consists of two steps: i) predicting the star-formation and chemical evolutionary histories of the high- z building blocks of the MW, i.e. the *MW progenitors*, using a data-constrained model; and ii) constructing the synthetic SEDs. In 2.1 we summarize the model employed and in 2.2 we explain how we infer the mock SEDs.

2.1. The Milky Way evolution model: NEFERTITI

We employ NEFERTITI (NEar FiEld cosmology: Re-Tracing Invisible Times, Koutsouridou et al. 2023), a state-of-the-art semi-analytical model for the formation and evolution of a MW-like galaxy that can be coupled with N-body simulations of dark matter (DM) only or with merger trees produced via Monte Carlo algorithms.

A MW analog is defined by the following physical properties of our Galaxy at $z = 0$: the virial mass $M_{vir} = (1.3 \pm 0.3) \times 10^{12} M_{\odot}$, the stellar mass $M_{\star} = (5 \pm 1) \times 10^{10} M_{\odot}$, and the star formation rate $SFR = 1 - 3 M_{\odot} yr^{-1}$ (e.g. Bland-Hawthorn & Gerhard 2016), the metallicity distribution function of halo stars (Bonifacio et al. 2021), the gas-to-stellar mass ratio $M_g/M_{\star} = 0.1 - 0.15$ (e.g. Ferrière 2001), and the metallicity of the dense, $Z_{ISM} \approx Z_{\odot}$, and diffuse gas, $Z_{IGM} \approx 0.1 - 0.3 Z_{\odot}$ (e.g. Tripp et al. 2003, for more details and references see Sec 2.3 of Koutsouridou et al. 2023.). Indeed, the model is calibrated to reproduce all these present-day observational properties of the MW.

NEFERTITI was developed from earlier semi-analytical models for the Local Group formation (Salvadori et al. 2007; Salvadori et al. 2015; Pagnini et al. 2023). Its main innovations are the treatment of the incomplete sampling of the stellar Initial Mass Function (IMF, see Rossi et al. 2021), the exploration of the unknown IMF of the first (Pop III) stars and the energy distribution function of the first supernovae (SNe, see Koutsouridou et al. 2024).

NEFERTITI tracks the evolution of baryonic matter inside the DM halos by accounting for star formation and feedback processes. Stars form with a rate proportional to the available gas mass in DM halos that reach a minimum mass value, which changes over time according to the evolution of the ionizing and photo-dissociating radiation (Salvadori & Ferrara 2009). Pop III stars initially form in the pristine gas, which is then enriched with metals from stellar winds and SNe. SNe explosions can eject a fraction of gas/metals mass outside of the MW progenitors, thus decreasing their star formation and enriching the intergalactic medium (IGM). Metals are assumed to be instantaneously mixed and when the metallicity of the interstellar medium reaches a value $Z_{gas} > 10^{-4.5} Z_{\odot}$ (de Bressan et al. 2017), normal (Pop II) stars form according to a Larson IMF (Larson 1998) with $m_{\star} = [0.1, 100] M_{\odot}$ and a peak at $m_{ch} = 0.35 M_{\odot}$.

Here we use NEFERTITI coupled with 50 different merger histories, to have a valid statistical sample. For each merger tree, there is a most massive progenitor (i.e. the MW major branch) and other 10^{2-4} smaller systems. For example, a typical MW major branch at $z = 11$ has stellar mass $M_{\star} \approx 10^7 M_{\odot}$ and gas metal-

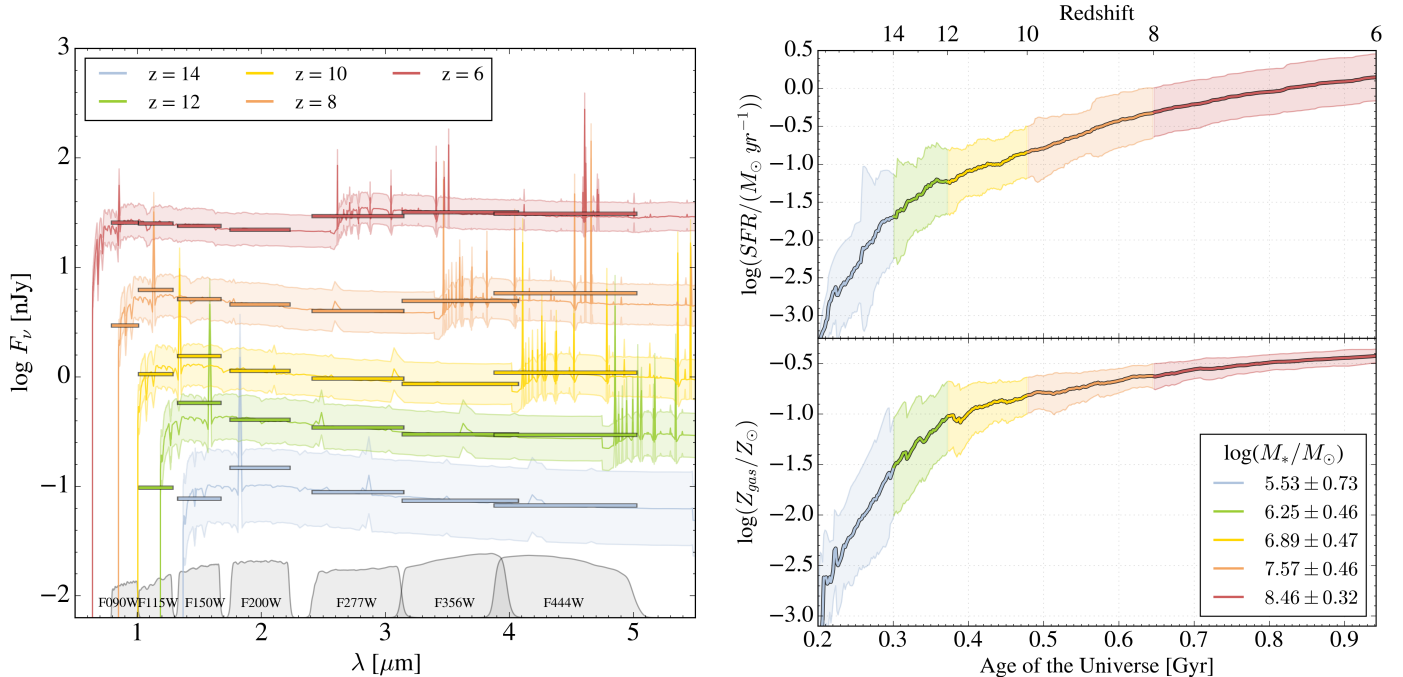


Figure 1. *Left:* Average synthetic SEDs for the MW major branch simulated by the NEFERTITI model, color-coded for redshift. For each mean SED, we show the corresponding photometries in the JWST NIRCcam filters. The shaded area represents the standard deviation due to the different merger tree realizations. *Right:* Average star-formation (top panel) and metal-enrichment histories (bottom panel) of the MW major branch, with the same color coding. On the bottom-right, we report the mean M_* at the redshifts shown on the left.

licity $Z_{gas} \approx 0.1 Z_\odot$, while the other progenitors can go down to $M_* \approx 10^2 M_\odot$ and $Z_{gas} \approx 10^{-4} Z_\odot$. For each of these halos, we have access to the star-formation and metal-enrichment histories sampled every Myr from $z = 18$ to $z = 6$. Here we adopt a Pop III Larson IMF with $m_* = [0.8, 1000] M_\odot$ and $m_{ch} = 10 M_\odot$, consistently with stellar archaeology observations (see Koutsouridou et al. 2023, 2024). However, our findings are independent of the assumed Pop III IMF.

2.2. Building Up Galaxy Spectra

To make accurate predictions for the emission of the MW progenitors at high- z , we build their synthetic SEDs using the spectral synthesis code Yggdrasil (Zackrisson et al. 2011) in the following manner. For each timestep of 1 Myr, consistently with the NEFERTITI code, we assume an instantaneous instance of star formation. Both the M_* formed and the Z_{gas} from which the stars form, are taken from the output of the galaxy-formation model. With these properties as input, the Yggdrasil code provides the rest-frame spectrum of a simple stellar population (SSP) at different ages (see Zackrisson et al. 2011 for more details). For Pop II stars, the available IMF is the Kroupa 2001 in the interval $m_* = [0.1 - 100] M_\odot$ and the SSP are from Starburst99 (Leitherer et al. 1999; Vázquez & Leitherer 2005). For

Pop III stars we choose the lognormal IMF option in the range $m_* = [1 - 500] M_\odot$ with the SSP from Raiter et al. 2010. The SEDs shown in this work will have a maximal nebular contribution, thus no escape of Lyman continuum photons, and no dust corrections.

To model the synthetic SED of the progenitor galaxy at a chosen redshift, we assemble the emitted rest-frame spectra of all the star-formation bursts that make up its evolutionary history and shift into the observed frame of reference. Fig. 1 (left) shows the average SED evolution of the MW major branch and the corresponding synthetic photometries in the JWST NIRCcam filters. On the right, we show the average SFR and Z_{gas} as a function of the cosmic time. The colors mark the redshifts at which the SED is shown.

3. RESULTS

3.1. Detectability of the MW Major Branch

We investigate the detectability of the most massive progenitor of the MW at different redshifts with JWST NIRCcam photometry. To this end, we select the major branch (MB) in each of the 50 merger trees simulated with NEFERTITI (see Sec. 2.1). More details on the possible evolution of a MB are in Appendix A. By modeling their SED evolution as shown in the example in Fig. 1, we can analyze the possible behavior

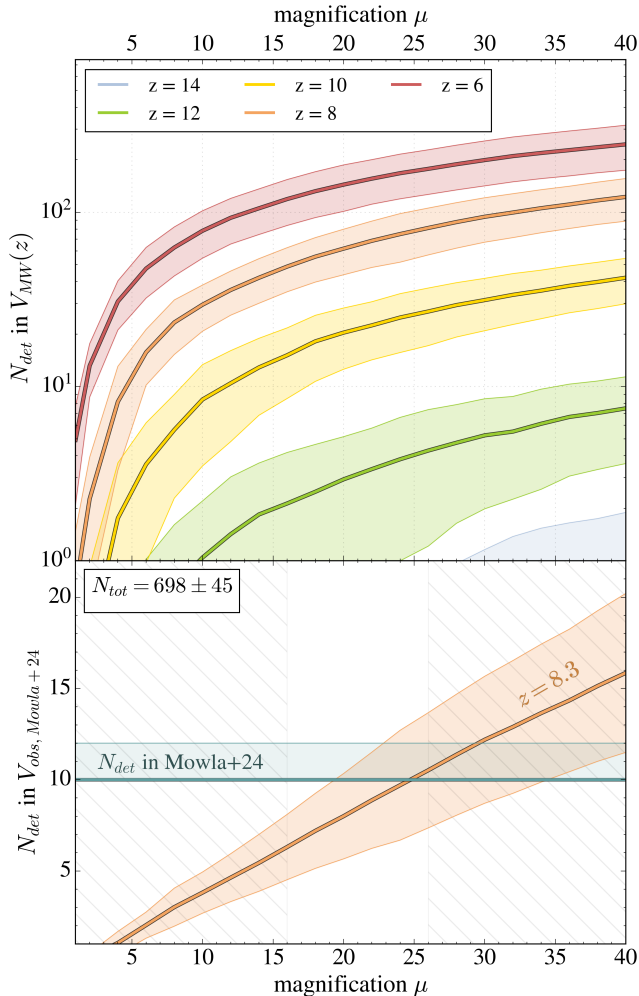


Figure 2. *Top:* Predictions for the number of detectable progenitors in the virial volume of the MW at different z , as a function of the magnification factor. From the 50 merger histories provided by the NEFERTITI model, we calculate the mean number of detections (solid lines) and the standard deviation (shaded areas). *Bottom:* Comparison between the number of systems detected in the Firefly Sparkle (dark green) and the number of progenitors predicted to be detectable in the same conditions (i.e. z , volume, lensing). The white area highlights the lensing range of the central region of the Firefly Sparkle.

of a typical MW-like galaxy at high- z . We determine the detectability by comparing the synthetic photometry of the MW major branches at different ages (using steps of $\Delta z = 0.1$) to the detection limits of typical deep JWST surveys in the NIRCcam wide filters. Since we do not include the IGM attenuation in our spectral synthesis, we ignore the detectability in the filters at $\lambda < \lambda_{obs}(\text{Ly}\alpha) \approx 1215(1+z)\text{\AA}$.

Considering the detection limits of the JADES survey (assuming the 5σ flux depths from Rieke et al. 2023), we predict that out of the 50 MW major branch real-

izations, one is detectable at $z = 11$, half at $z = 8.2$ and all at $z = 7.1$. From this simple analysis, we conclude that the probability for a MW-like progenitor to become detectable in a deep JWST survey like JADES is $P_{det}^{MB}(z < 11) \geq 2\%$, $P_{det}^{MB}(z < 8.2) \geq 50\%$, and $P_{det}^{MB}(z < 7.1) = 100\%$

3.2. Detectability of a MW-type Assembly

We have shown that a typical MW progenitor can become detectable and appear in JWST observations from $z \lesssim 8$. However, to interpret an observed galaxy as a MW-like progenitor we need to make further predictions on its expected environment and properties. Indeed, we expect the most massive MW progenitor at high- z to be surrounded by hundreds of smaller galaxies, which will accrete and merge over time. Due to their lower masses and weaker emission, we likely need to rely on gravitational lensing to be able to observe such a group of smaller MW building blocks. Here, we investigate their detectability in a typical JWST lensing survey.

By applying the method used in Sec. 3.1 for the most massive progenitor to *all* the MW progenitors predicted by NEFERTITI, we predict the number of MW building blocks that we expect to be detectable for different observational conditions, i.e. as a function of redshift (z), observed volume (V_{obs}), and magnification factor (μ). The threshold for detectability is set according to the JWST NIRCcam detection limits of the CANUCS program (Willott et al. 2022).

Fig. 2 (top panel) shows our predictions at different z for the number of MW progenitors detectable in a JWST lensing survey as a function of μ , within the MW volume, which can be estimated as:

$$V_{MW}(z) = \frac{4}{3}\pi \left(\frac{R_{MW}^{vir}(0)}{(1+z)} \right)^3 \quad (1)$$

where $R_{MW}^{vir}(0) \approx 240$ kpc. Without gravitational lensing (i.e. $\mu = 1$) we can detect only one progenitor at $z = 8$, as estimated in Sec. 3.1, and up to ≈ 5 MW progenitors at $z = 6$. In general, we see an increasing number of detections both for bigger μ and for lower z , understanding the importance of lensing when aiming to observe the MW assembly at high- z .

Our predictions can be easily applied and compared to specific JWST observations to understand if they can be interpreted as MW-like systems, by simply rescaling the MW volume to the one observed:

$$N_{det}(z) = N_{det,MW}(z) \frac{V_{obs}(z)}{V_{MW}(z)}. \quad (2)$$

Let us apply this to the Firefly Sparkle observation. For the observed region V_{obs} we assume a sphere with

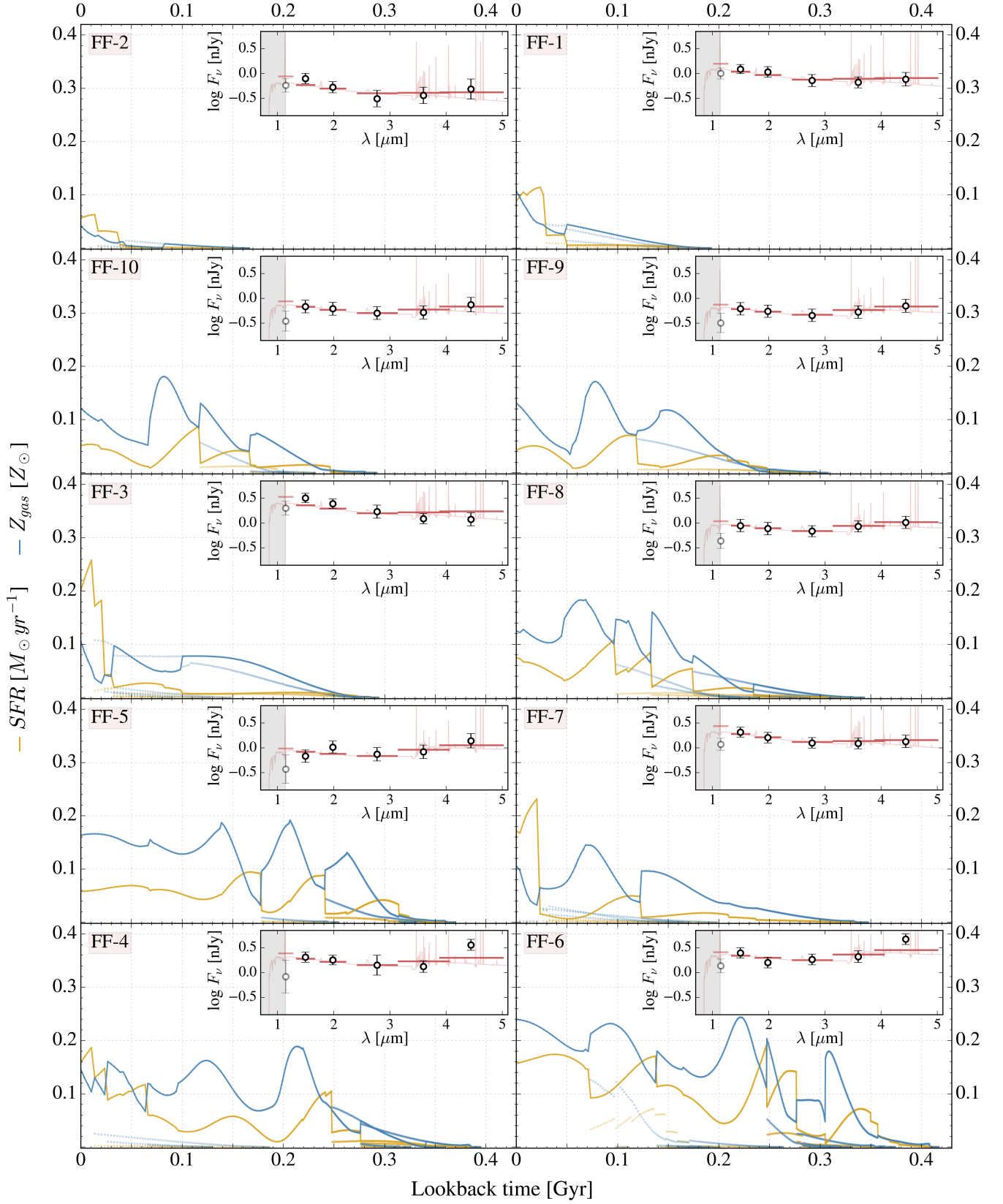


Figure 3. Star-formation (gold) and metal-enrichment (blue) histories of the progenitors that best fit the emission of each system of the Firefly Sparkle, in order of increasing estimated M_{\star} . The synthetic SED is shown in the top-right inset (red), together with the Mowla et al. 2024 observations (black). The grey areas are not included in the fit. The histories of the minor branches (dotted lines) that have merged with the most massive progenitor (solid lines) to form the final one at $z = 8.3$ are also shown.

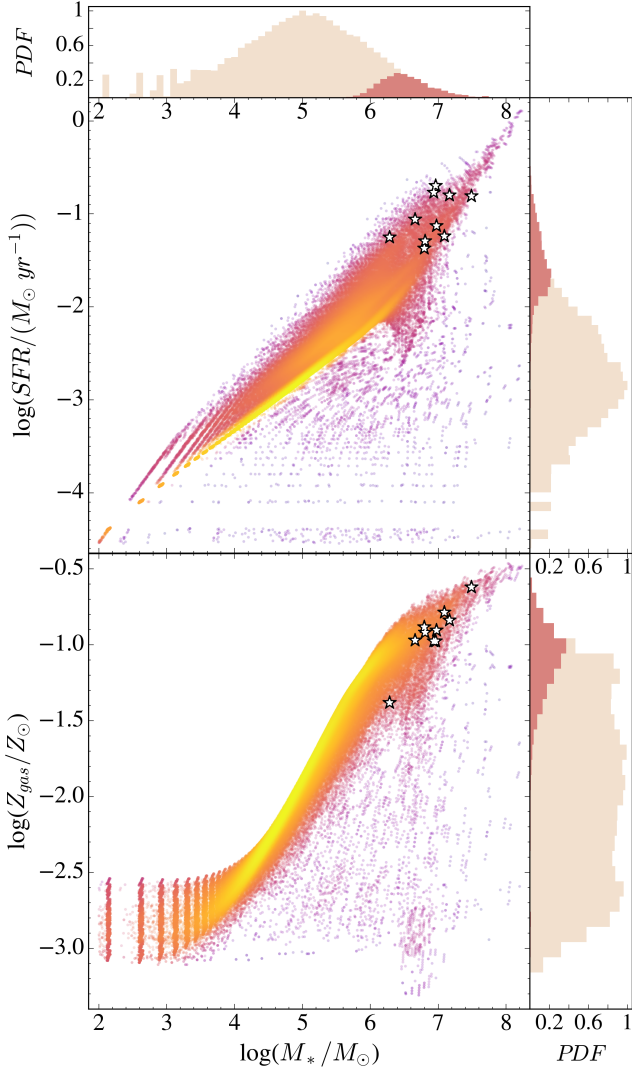


Figure 4. SFR (top panel) and Z_{gas} (bottom panel) as a function of M_* for all the MW progenitors predicted by the NEFERTITI model at $z = 8.3$, colored by density of points. The best-fitting progenitors to the Firefly Sparkle are highlighted with star markers. On top and the sides, we show the probability distribution functions (PDF) of the properties of all the progenitors (beige) and the detectable ones (red), assuming $\mu = 24$ and the detection limits of CANUCS (Willott et al. 2022)

$R_{obs} = 13$ kpc, corresponding to the estimated distance of the second-closest galaxy to the Firefly Sparkle.

In Fig. 2 (bottom) we show the comparison between the number of systems detected by Mowla et al. 2024 (grey), consisting of 10 systems in the central region and two nearby galaxies, and our predictions for the same observational conditions (orange). We find that in the magnification range observed in the Firefly Sparkle, $\mu = 16 - 26$, our predicted number of detectable MW progenitors is consistent with those observed. Although

this is just a rough estimate, the remarkable consistency of our predictions with the observed number of sources provides a solid groundwork for their interpretation as MW-like building blocks, i.e. galaxies. In the next section, we will compare the systems of the Firefly Sparkle one by one to our modeled galaxies.

3.3. Interpreting the Firefly Sparkle

Here we present the properties of the individual Firefly Sparkle systems inferred through forward modeling with the MW galaxy-formation model NEFERTITI. We construct the synthetic SEDs of the MW building blocks according to their star-formation and metal-enrichment histories (see Sec. 2.2).

With this method, we build ≈ 35000 mock JWST NIRCam photometric data sets, representing 50 different possible populations of MW progenitors at $z = 8.3$. Among them, we select the 10 galaxies whose synthetic photometry best fits the observational data of the 10 Firefly Sparkle systems. To this end, we assume the μ estimated in Mowla et al. 2024 for each “star cluster” to retrieve its unlensed photometry and compare it to our synthetic SEDs, selecting the one with the minimum reduced χ^2 value. We only consider the central Firefly Sparkle, since we don’t have the photometric data of the two nearby galaxies.

Fig. 3 shows the star formation and metal enrichment histories for the ten best-fitting MW progenitors, from the least (top-left) to the most (bottom-right) massive. The insets show the correspondent synthetic SEDs, compared to the photometric JWST data. The emission of the MW building blocks predicted by NEFERTITI at $z = 8.3$ is in good agreement with the photometric data of the Firefly Sparkle, with $\chi_r^2 < 1.4$. We notice that the SFHs of the MW progenitors are not smooth and regular but rather stochastic and characterized by multiple bursts and drops of star formation due to feedback processes (see Sec. 2.1). These realistic complex star formation and metal enrichment histories can fit remarkably well the observed emission of all the observed $z = 8.3$ systems *simultaneously*, proving that we can interpret the Firefly Sparkle as a MW-like assembly.

Table 1 reports the physical properties inferred for the 10 Firefly Sparkle systems, which in our interpretation are MW-progenitor galaxies. Their stellar masses are $M_* = 10^{6.2-7.5} M_\odot$, their DM halos have $M_h = 10^{8.1-9} M_\odot$, the instantaneous $SFR = 0.04 - 0.20 M_\odot yr^{-1}$, and $Z_{gas} = 0.04 - 0.24 Z_\odot$. We also report t_{half} , defined as the time needed to form half of the total stellar mass, which is of the order of 150–300 Myr.

Table 1. Properties of the Firefly Sparkle systems inferred via forward modeling with NEFERTITI.

Name	$\log(M_*)$ [M_\odot]	$\log(SFR)$ [$M_\odot \text{ yr}^{-1}$]	$\log(Z_{gas})$ [Z_\odot]	$\log(M_h)$ [M_\odot]	t_{half} [Myr]	$\min \chi_r^2$
FF-1	6.64 ± 0.09	-1.06 ± 0.13	-0.97 ± 0.15	8.35 ± 0.08	169 ± 45	0.232
FF-2	6.26 ± 0.10	-1.25 ± 0.16	-1.38 ± 0.14	8.14 ± 0.08	150 ± 47	0.340
FF-3	6.95 ± 0.06	-0.70 ± 0.10	-0.98 ± 0.11	8.60 ± 0.04	267 ± 37	1.367
FF-4	7.16 ± 0.07	-0.80 ± 0.06	-0.84 ± 0.06	8.74 ± 0.05	309 ± 31	0.900
FF-5	7.08 ± 0.08	-1.24 ± 0.14	-0.79 ± 0.14	8.68 ± 0.07	220 ± 31	0.407
FF-6	7.48 ± 0.03	-0.81 ± 0.04	-0.62 ± 0.03	8.98 ± 0.02	288 ± 31	0.809
FF-7	6.93 ± 0.09	-0.77 ± 0.09	-0.98 ± 0.07	8.57 ± 0.07	320 ± 43	0.092
FF-8	6.96 ± 0.07	-1.13 ± 0.16	-0.90 ± 0.21	8.64 ± 0.06	241 ± 35	0.002
FF-9	6.78 ± 0.07	-1.37 ± 0.27	-0.88 ± 0.27	8.48 ± 0.05	199 ± 37	0.027
FF-10	6.80 ± 0.07	-1.29 ± 0.24	-0.92 ± 0.24	8.50 ± 0.05	180 ± 35	0.057

As a result, these galaxies have old stellar populations that have formed more than 100 Myr before the observation.

In Fig. 4 we show the properties of all the $z = 8.3$ MW building blocks in 50 realizations of NEFERTITI. On the top and right panels, we can visualize the probability distribution of their properties, where we have highlighted in red those of the galaxies that can be detected in the observational conditions of Mowla et al. 2024 and assuming $\mu = 24$ (for different μ see Appendix B). The detectable MW progenitors are the most massive, star-forming, and metal-rich systems, meaning that we are observing only a biased sample. The star markers show the galaxies that best fit the individual Firefly Sparkle systems, which are scattered across the observable regions.

Here we show all the 50 merger tree realizations to visualize the possible properties of a MW-assembly environment at $z = 8.3$. If we focus on a single assembling history, only a couple of galaxies are more massive and star-forming than our best fits. They could be the two nearby galaxies, but we need further photometric observations to conclude their interpretation.

4. DISCUSSION AND CONCLUSIONS

The recent JWST CANUCS observation of the Firefly Sparkle claimed to be a MW-like galaxy assembly at $z \approx 8$, presented us with the unique opportunity to connect the still debated early stages of galaxy formation to our knowledge of the Local Universe. In this Letter, we performed forward modeling of the MW progenitors with the galaxy-formation model NEFERTITI to make both predictions and interpretations for JWST. We chose to use Monte Carlo merger trees to have a valid

statistical sample of different possible merger histories for the Milky Way.

First, analyzing the multiple realizations of possible MW assembly histories, we find that the most massive MW progenitor can appear within JADES detection limits as early as $z \approx 11$ (2% probability), it is very likely detectable at $z \approx 8.2$ (50%), and always detectable at $z \leq 7.1$. As a result of this prediction, in both completed and ongoing deep surveys of JWST, we could have observed the major branch of MW-like galaxies that still require interpretation.

Second, we confirm the interpretation of the Firefly Sparkle as a MW analog. The number of systems detected in Mowla et al. 2024 is indeed consistent with the predicted number of detectable MW progenitors assuming the same observational conditions. Moreover, the NIRCcam photometric data of the 10 Firefly Sparkle “star clusters” are in good agreement with the synthetic photometries of the MW progenitors at the same redshift, with $\chi_r^2 < 1.4$. By identifying the MW building blocks in NEFERTITI that best fit the observations, we estimate the physical properties of each of these systems, which are not predicted to be star clusters but rather MW progenitor *galaxies* with $M_h = 10^{8.1-9} M_\odot$, $M_* = 10^{6.2-10^{7.5}} M_\odot$, $SFR = 0.04 - 0.20 M_\odot \text{ yr}^{-1}$ and $Z_{gas} = 0.04 - 0.24 Z_\odot$.

The stellar masses inferred by Mowla et al. 2024 with spectrophotometric fitting techniques (Iyer & Gawiser 2017; Iyer et al. 2019), $M_{*,obs} = 10^{5.3-5.8} M_\odot$, are on average lower than our predictions. This is not surprising given the bursty and long SFHs of our MW progenitors, with $t_{half} = 150 - 300$ Myr. Indeed, reconstructing and resolving old stellar populations through SED fitting is particularly difficult due to the outshining of their stel-

lar emission by the dominating nebular emission from young stars (e.g. Whitler et al. 2023; Giménez-Arteaga et al. 2024). However, if we self-consistently calculate the SFR values from the specific $SFRs$ reported in the Firefly Sparkle paper, and their respective errors, we find $SFR_{obs} = 0.003 - 0.6 M_{\odot} yr^{-1}$, which are consistent with our estimates.

As for the gas metallicity, Mowla et al. (2024) derive a single value for the entire system, $Z_{gas,obs} = 0.02 \pm 0.01 Z_{\odot}$. We find the Z_{gas} and its evolution for each MW progenitor, with values that are higher than their estimation but still subsolar. The reason for this discrepancy could be due to the direct T_e method used to infer Z_{gas} from the observed spectrum. By fitting the observations with the HOMERUN code (Marconi et al. 2024), which uses a weighted combination of multiple single-cloud photoionization models, we found a total metallicity value that is consistent with those predicted by the NEFERTITI model.

In conclusion, our results show that the Firefly Sparkle observation is consistent with what we predict for a

MW-like environment at $z = 8.3$. Our forward modeling approach has allowed us to estimate the properties of the individual MW building blocks with physically motivated and complex evolutionary histories. To help ongoing and future JWST surveys understand if they are witnessing high- z MW-like environments in lensed fields, we provide predictions for the number of detectable MW progenitors at various redshifts and for different magnification factors. Catching other MW-like systems at cosmic dawn will indeed allow the community to collect different pictures of a MW-analog during its infancy. Ultimately, more JWST observations combined with our predictions might allow us to link the high- and the low- z perspectives to understand the early assembly stages of our Galaxy.

ACKNOWLEDGEMENTS

This project received funding from the ERC Starting Grant NEFERTITI H2020/804240 (PI: Salvadori).

REFERENCES

- Bland-Hawthorn, J., & Gerhard, O. 2016, *ARA&A*, 54, 529, doi: [10.1146/annurev-astro-081915-023441](https://doi.org/10.1146/annurev-astro-081915-023441)
- Bonifacio, P., Monaco, L., Salvadori, S., et al. 2021, *A&A*, 651, A79, doi: [10.1051/0004-6361/202140816](https://doi.org/10.1051/0004-6361/202140816)
- Buder, S., Sharma, S., Kos, J., et al. 2021, *MNRAS*, 506, 150, doi: [10.1093/mnras/stab1242](https://doi.org/10.1093/mnras/stab1242)
- Carniani, S., Hainline, K., D'Eugenio, F., et al. 2024, arXiv e-prints, arXiv:2405.18485, doi: [10.48550/arXiv.2405.18485](https://doi.org/10.48550/arXiv.2405.18485)
- de Bennassuti, M., Salvadori, S., Schneider, R., Valiante, R., & Omukai, K. 2017, *MNRAS*, 465, 926, doi: [10.1093/mnras/stw2687](https://doi.org/10.1093/mnras/stw2687)
- Eisenstein, D. J., Willott, C., Alberts, S., et al. 2023, arXiv e-prints, arXiv:2306.02465, doi: [10.48550/arXiv.2306.02465](https://doi.org/10.48550/arXiv.2306.02465)
- Endsley, R., Stark, D. P., Whitler, L., et al. 2023, arXiv e-prints, arXiv:2306.05295, doi: [10.48550/arXiv.2306.05295](https://doi.org/10.48550/arXiv.2306.05295)
- Ferrière, K. M. 2001, *Reviews of Modern Physics*, 73, 1031, doi: [10.1103/RevModPhys.73.1031](https://doi.org/10.1103/RevModPhys.73.1031)
- Finkelstein, S. L., Bagley, M. B., Ferguson, H. C., et al. 2023, *ApJL*, 946, L13, doi: [10.3847/2041-8213/acade4](https://doi.org/10.3847/2041-8213/acade4)
- Gaia Collaboration, Vallenari, A., Brown, A. G. A., et al. 2023, *A&A*, 674, A1, doi: [10.1051/0004-6361/202243940](https://doi.org/10.1051/0004-6361/202243940)
- Gelli, V., Salvadori, S., Ferrara, A., Pallottini, A., & Carniani, S. 2023, *ApJL*, 954, L11, doi: [10.3847/2041-8213/acee80](https://doi.org/10.3847/2041-8213/acee80)
- Giménez-Arteaga, C., Fujimoto, S., Valentino, F., et al. 2024, *A&A*, 686, A63, doi: [10.1051/0004-6361/202349135](https://doi.org/10.1051/0004-6361/202349135)
- Harikane, Y., Ouchi, M., Oguri, M., et al. 2023, *ApJS*, 265, 5, doi: [10.3847/1538-4365/acaaa9](https://doi.org/10.3847/1538-4365/acaaa9)
- Harikane, Y., Inoue, A. K., Ellis, R. S., et al. 2024, arXiv e-prints, arXiv:2406.18352, <https://arxiv.org/abs/2406.18352>
- Hartwig, T., Magg, M., Chen, L.-H., et al. 2022, *ApJ*, 936, 45, doi: [10.3847/1538-4357/ac7150](https://doi.org/10.3847/1538-4357/ac7150)
- Iyer, K., & Gawiser, E. 2017, *ApJ*, 838, 127, doi: [10.3847/1538-4357/aa63f0](https://doi.org/10.3847/1538-4357/aa63f0)
- Iyer, K. G., Gawiser, E., Faber, S. M., et al. 2019, *ApJ*, 879, 116, doi: [10.3847/1538-4357/ab2052](https://doi.org/10.3847/1538-4357/ab2052)
- Koutsouridou, I., Salvadori, S., & Skúladóttir, Á. 2024, *ApJL*, 962, L26, doi: [10.3847/2041-8213/ad2466](https://doi.org/10.3847/2041-8213/ad2466)
- Koutsouridou, I., Salvadori, S., Skúladóttir, Á., et al. 2023, *MNRAS*, 525, 190, doi: [10.1093/mnras/stad2304](https://doi.org/10.1093/mnras/stad2304)
- Kroupa, P. 2001, *MNRAS*, 322, 231, doi: [10.1046/j.1365-8711.2001.04022.x](https://doi.org/10.1046/j.1365-8711.2001.04022.x)
- Langeroodi, D., & Hjorth, J. 2024, arXiv e-prints, arXiv:2404.13045, doi: [10.48550/arXiv.2404.13045](https://doi.org/10.48550/arXiv.2404.13045)
- Larson, R. B. 1998, *Monthly Notices of the Royal Astronomical Society*, 301, 569
- Leitherer, C., Schaerer, D., Goldader, J. D., et al. 1999, *ApJS*, 123, 3, doi: [10.1086/313233](https://doi.org/10.1086/313233)

- Looser, T. J., D'Eugenio, F., Maiolino, R., et al. 2023, arXiv e-prints, arXiv:2306.02470, doi: [10.48550/arXiv.2306.02470](https://doi.org/10.48550/arXiv.2306.02470)
- Marconi, A., Amiri, A., Feltre, A., et al. 2024, arXiv e-prints, arXiv:2401.13028, doi: [10.48550/arXiv.2401.13028](https://doi.org/10.48550/arXiv.2401.13028)
- Mowla, L., Iyer, K., Asada, Y., et al. 2024, arXiv e-prints, arXiv:2402.08696, doi: [10.48550/arXiv.2402.08696](https://doi.org/10.48550/arXiv.2402.08696)
- Pagnini, G., Salvadori, S., Rossi, M., et al. 2023, MNRAS, 521, 5699, doi: [10.1093/mnras/stad912](https://doi.org/10.1093/mnras/stad912)
- Pallottini, A., & Ferrara, A. 2023, A&A, 677, L4, doi: [10.1051/0004-6361/202347384](https://doi.org/10.1051/0004-6361/202347384)
- Raiter, A., Schaerer, D., & Fosbury, R. A. E. 2010, A&A, 523, A64, doi: [10.1051/0004-6361/201015236](https://doi.org/10.1051/0004-6361/201015236)
- Rieke, M. J., Robertson, B., Tacchella, S., et al. 2023, ApJS, 269, 16, doi: [10.3847/1538-4365/acf44d](https://doi.org/10.3847/1538-4365/acf44d)
- Roberts-Borsani, G., Treu, T., Chen, W., et al. 2023, Nature, 618, 480, doi: [10.1038/s41586-023-05994-w](https://doi.org/10.1038/s41586-023-05994-w)
- Rossi, M., Salvadori, S., & Skúladóttir, Á. 2021, Monthly Notices of the Royal Astronomical Society
- Salvadori, S., & Ferrara, A. 2009, MNRAS, 395, L6, doi: [10.1111/j.1745-3933.2009.00627.x](https://doi.org/10.1111/j.1745-3933.2009.00627.x)
- Salvadori, S., Ferrara, A., Schneider, R., Scannapieco, E., & Kawata, D. 2010, Monthly Notices of the Royal Astronomical Society: Letters, 401, L5
- Salvadori, S., Schneider, R., & Ferrara, A. 2007, Monthly Notices of the Royal Astronomical Society, 381, 647
- Salvadori, S., Skúladóttir, Á., & Tolstoy, E. 2015, MNRAS, 454, 1320, doi: [10.1093/mnras/stv1969](https://doi.org/10.1093/mnras/stv1969)
- Sun, G., Faucher-Giguère, C.-A., Hayward, C. C., & Shen, X. 2023, MNRAS, 526, 2665, doi: [10.1093/mnras/stad2902](https://doi.org/10.1093/mnras/stad2902)
- Treu, T., Roberts-Borsani, G., Bradac, M., et al. 2022, ApJ, 935, 110, doi: [10.3847/1538-4357/ac8158](https://doi.org/10.3847/1538-4357/ac8158)
- Tripp, T. M., Wakker, B. P., Jenkins, E. B., et al. 2003, AJ, 125, 3122, doi: [10.1086/374995](https://doi.org/10.1086/374995)
- Tumlinson, J. 2010, ApJ, 708, 1398, doi: [10.1088/0004-637X/708/2/1398](https://doi.org/10.1088/0004-637X/708/2/1398)
- Vanzella, E., Claeysens, A., Welch, B., et al. 2023, ApJ, 945, 53, doi: [10.3847/1538-4357/acb59a](https://doi.org/10.3847/1538-4357/acb59a)
- Vázquez, G. A., & Leitherer, C. 2005, ApJ, 621, 695, doi: [10.1086/427866](https://doi.org/10.1086/427866)
- White, S. D. M., & Rees, M. J. 1978, MNRAS, 183, 341, doi: [10.1093/mnras/183.3.341](https://doi.org/10.1093/mnras/183.3.341)
- Whitler, L., Stark, D. P., Endsley, R., et al. 2023, MNRAS, 519, 5859, doi: [10.1093/mnras/stad004](https://doi.org/10.1093/mnras/stad004)
- Willott, C. J., Doyon, R., Albert, L., et al. 2022, Publ. Astr. Soc. Pac., 134, 025002, doi: [10.1088/1538-3873/ac5158](https://doi.org/10.1088/1538-3873/ac5158)
- Zackrisson, E., Rydberg, C.-E., Schaerer, D., Östlin, G., & Tuli, M. 2011, ApJ, 740, 13, doi: [10.1088/0004-637X/740/1/13](https://doi.org/10.1088/0004-637X/740/1/13)

APPENDIX

A. PROPERTIES OF THE MW MAJOR BRANCHES

The 50 merger tree realizations of the NEFERTITI model provide us with 50 different possible formation histories of the MW major branches. Fig. 5 shows the evolution of the physical properties (i.e. M_h , M_* , SFR , Z_{gas}) for each merger tree’s most massive MW progenitor, from $z \approx 18$ to $z \approx 6$. The wide range of possible evolutions showcases the importance of using the DM merger tree method (e.g. see Salvadori et al. 2007, for more details), which allows us to have a significant statistical sample. We can notice how the SFR evolves in a stochastic and bursty manner due to the stellar feedback (see Sec. 2.1 and Koutsouridou et al. 2023, for more details on NEFERTITI) and to the galaxy merger process, clearing once more the importance of using physically-motivated SFHs when interpreting JWST observations at high- z .

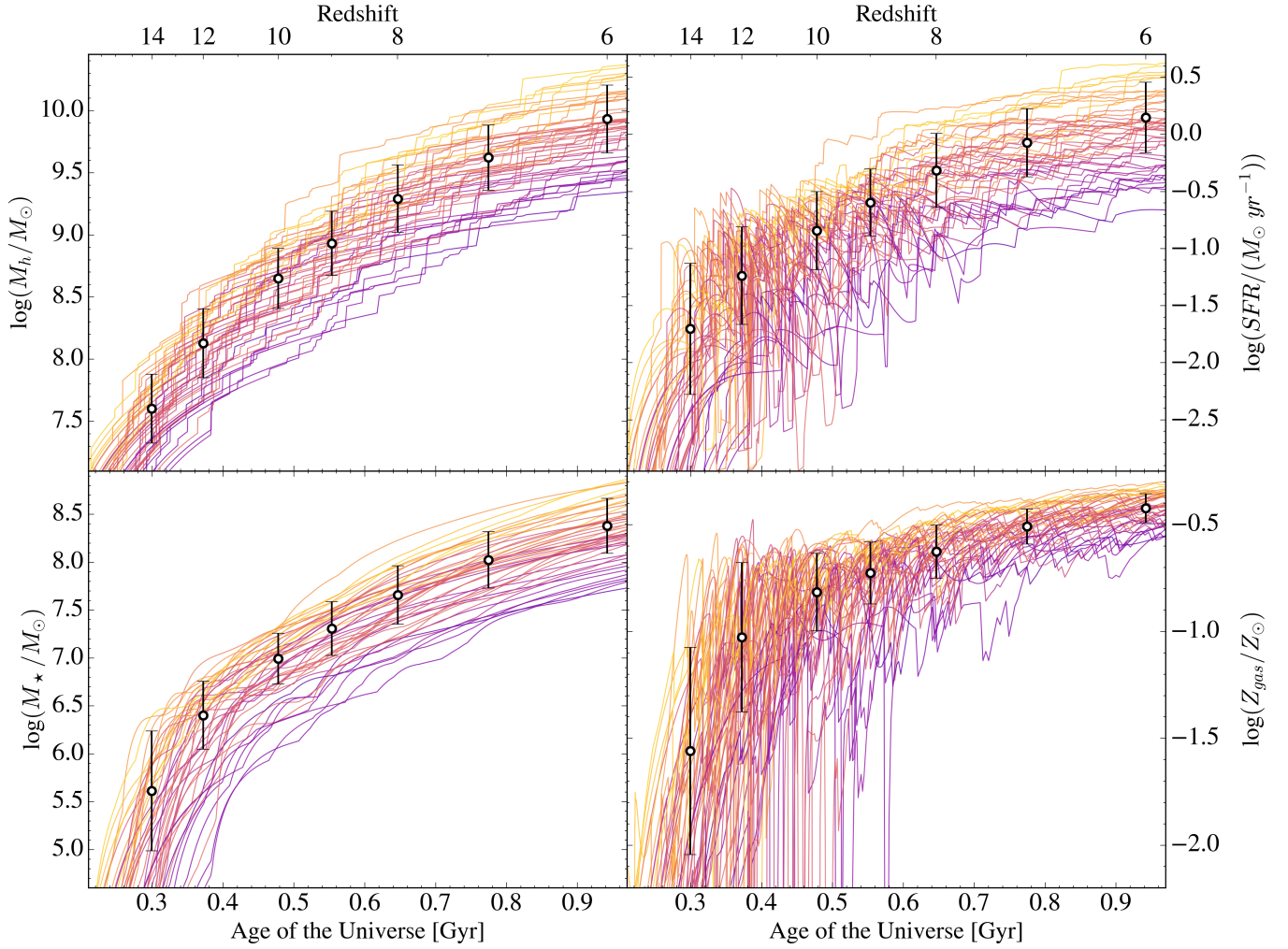


Figure 5. Physical properties of all the MW major branches simulated by NEFERTITI: halo mass (top left), stellar mass (bottom left), star formation rate (top right), and gas metallicity (bottom right), colored by halo mass at $z = 6$. The black error bars represent the mean value and the relative standard deviation at $z = 14, 12, 10, 9, 8, 7, 6$.

B. DETECTABLE MW PROGENITORS WITH DIFFERENT LENSINGS

In Sec. 3.3 we found that the MW-progenitor galaxies that can be detected in a JWST lensing survey like CANUCS (Willott et al. 2022) are in the high-tail of the M_* , SFR , and Z_{gas} distributions. To better visualize the detectable

galaxies, in Fig. 6 we show the final properties of all the MW progenitors at $z = 8.3$ for 50 merger histories, with each point representing a progenitor galaxy. In this way, we can highlight the single galaxies that can be detected at different μ . We notice that there are $SFR - M_*$ and $Z_{gas} - M_*$ relations for the detectability:

$$\log(SFR) \gtrsim -\log(M_*) + a(\mu) \quad (\text{B1})$$

$$\log(Z_{gas}) \lesssim 2\log(M_*) + b(\mu). \quad (\text{B2})$$

These relations quantify how we can observe lower-mass systems if they are more star-forming or metal-poor, and how a higher magnification factor can help us access more typical MW progenitor galaxies.

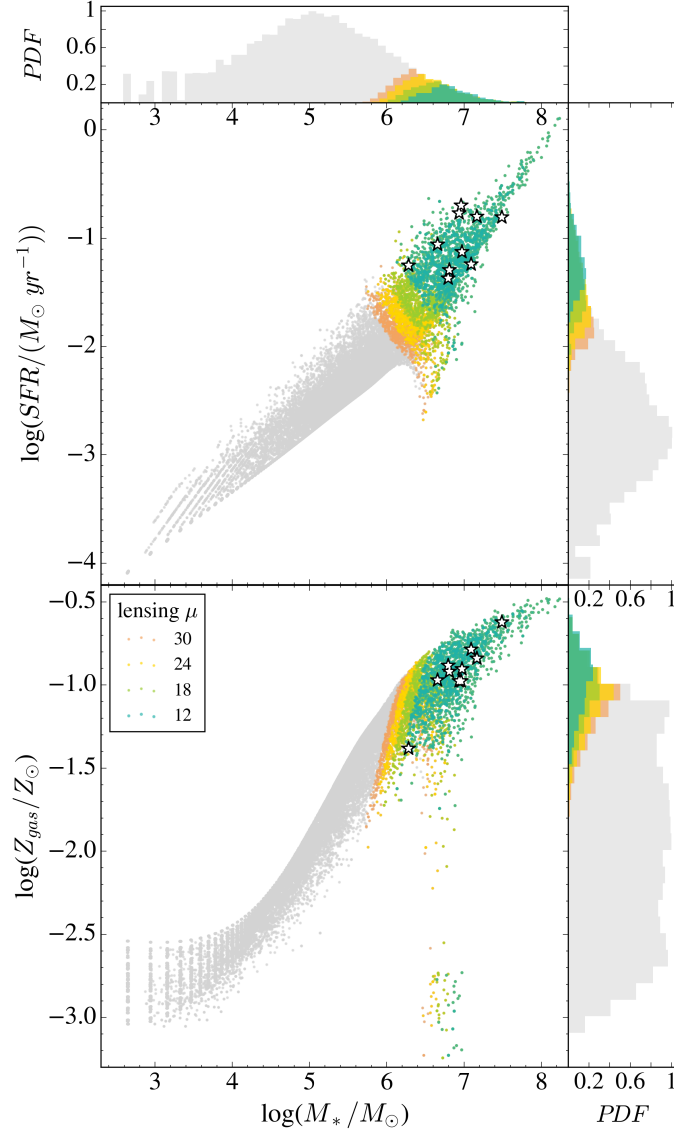


Figure 6. SFR (top panel) and Z_{gas} (bottom panel) as a function of M_* for all the MW progenitors predicted by the NEFERTITI model at $z = 8.3$. Assuming the detection limits of CANUCS (Willott et al. 2022), the grey points represent the non-detectable systems, while the colored ones are detectable with different magnification factors (i.e. orange for $\mu = 30$, yellow for $\mu = 24$, light green for $\mu = 18$ and dark green for $\mu = 12$). The best-fitting progenitors to the Firefly Sparkle are highlighted with star markers. On top and the sides, we show the probability distribution functions (PDF) of the properties of all the progenitors and of the detectable ones, again color-coded for μ .